Some new progress on the light absorption properties of linear alkyl benzene solvent *

Guang-You Yu(于广友)[1] De-Wen Cao(曹德文)[1] Ai-Zhong Huang(黄爱忠)[2]
Lei Yu(虞磊)[3] Chang-Wei Loh(罗章维)[1] Wen-Wen Wang(王文文)[1]
Zhi-Qiang Qian(钱志强)[1] Hai-Bo Yang(杨海波)[1] Huang Huang(黄璜)[1]
Zong-Qiang Xu(徐宗强)[1] Xue-Yuan Zhu(朱学园)[1] Bin Xu(徐斌)[1] Ming Qi(祁鸣)[1;1)]

[1] National Laboratory of Solid State Microstructures and School of Physics, Nanjing University, Nanjing 210093, China
[2] Jinling Petrochemical Corporation Ltd, Nanjing 210000, China
[3] National 863 Program New Material MO Precursors R&D Center, Nanjing University, Nanjing 210093, China

Abstract: Linear alkyl benzene (LAB) will be used as the solvent in a liquid scintillator mixture for the JUNO antineutrino experiment. Its light absorption properties should therefore be understood prior to its effective use in the experiment. Attenuation length measurements at a light wavelength of 430 nm have been performed on samples of LAB prepared for the JUNO experiment. Inorganic impurities in LAB have also been studied for their possibilities of light absorption in our wavelength of interest. In view of a tentative plan by the JUNO collaboration to utilize neutron capture with hydrogen in the detector, we also present in this work a preliminary study on the carbon–hydrogen ratio and the attenuation length of the samples.

Keywords: linear alkyl benzene (LAB), attenuation length, inorganic impurities, carbon–hydrogen ratio

PACS: 29.40.Mc, 78.30cb **DOI:** 10.1088/1674-1137/40/1/016002

1 Introduction

The Jiangmen Underground Neutrino Observatory (JUNO) is a multi-purpose experiment scheduled to start data-taking in 2020, with one of its aims being to study the neutrino mass hierarchy [1–4] for any physics beyond the Standard Model. As antineutrinos interact weakly with other particles, the JUNO detector needs to be large in size and consequently needs about 20 kilotons of linear alkyl benzene (LAB) as a liquid scintillator (LS) solvent. PPO and bis-MSB will be used as the solutes.

The sheer size of the detector poses a challenge in that the liquid scintillator to be used in the detector for the purpose of reacting with incoming antineutrinos is required to have high optical transparency and an attenuation length comparable to the size of the detector itself. Otherwise, photons emitted through a series of interactions between the antineutrinos and LS will be absorbed by the LS itself before reaching the photomultiplier tubes (PMTs) outside the JUNO detector. As the inner sphere of the JUNO central detector, which will contain the liquid scintillator, has a diameter of about 34 m, the attenuation length of the LAB solvent itself should be comparable to the said diameter, in order to prepare a liquid scintillator with minimal absorption of the emitted photons. The LAB currently in use in the Daya Bay detector [5] has an attenuation length about 10 m or slightly larger, which is still less than the requirement of JUNO.

It is imperative, therefore, that LAB with better light absorption properties is produced. To date, Goett et al. [6] and Ding et al. [7] have studied the attenuation length of LAB purified and prepared in the laboratory, with the former obtaining an attenuation length of 28.6 m and the latter obtaining 26 m from their respective samples. Looking forward, these results indicate that the aim to prepare LAB with an attenuation length of at least 30 m and comparable to the size of the JUNO detector is an achievable feat in the near future. In this work, we present a study on the light absorption properties of new LAB samples obtained through a scalable LAB manufacturing process from Jinling Petrochemical Corporation Ltd (hereafter known as “Jinling”) which can be feasibly used for mass production of LAB as required by the JUNO detector in future. The attenuation length of the samples has been measured using an updated setup with improved techniques that differ from those used for the Daya Bay experiment [8]. The largest

Received 21 April 2015, Revised 27 August 2015
∗ Supported by China Ministry of Science and Technology(2013CB834300)
1) E-mail: qming@nju.edu.cn

attenuation length as measured from our samples was found to be 26.8±0.4 m.

In addition, we have used an ICP-MS method to study the inorganic impurities in LAB, in contrast with the GC-MS and LC-MS methods used to study the organic impurities in Refs. [8, 9]. At present, we find the concentration of inorganic impurities to be so low that any influence on the LAB attenuation length can be provisionally ignored. The C/H ratio of LAB and a comparison between the samples based on their ratios has also been investigated. Based on the C/H ratio results and the corresponding attenuation length of LAB, we find that it is possible to prepare a LAB sample with large attenuation length while having a low C/H ratio.

The results of this work and the setup described herein will be useful for future studies in the preparation of LAB and finally LS with the stringent requirements for the light absorption properties needed by JUNO.

2 LAB samples

The LAB samples used in this work, tagged as NJ25#, NJ26#, NJ28#, NJ29#, NJ30#, NJ32# and NJ33#, were provided by Jinling. Specifically, NJ29#, NJ30#, NJ32# and NJ33# were prepared with some improved techniques that can help form a basis for large-scale manufacturing of LAB with large attenuation length in Jinling. NJ28# is a sample taken from the LS used in the Daya Bay detector, doped with PPO, bis-MSB and gadolinium (Gd). A sample of LAB without the addition of PPO, bis-MSB and Gd, tagged as NJ22#, originally prepared for the Daya Bay experiment, will be used as a reference in this work.

3 Attenuation length of LAB

3.1 Definition

The attenuation length L_λ is defined to be the distance in a material where the intensity of an incident light with wavelength λ is reduced by 1/e. This can be expressed as

$$I=I_0 e^{-\frac{x}{L_\lambda}}, \tag{1}$$

where I is the light intensity after it passes through the material, which in this work will be the LAB liquid, for a total path length x; I_0 is the initial light intensity.

3.2 Experimental setup

In this work, a 1.2 m steel tube with Teflon-covered inner wall was filled with LAB. A photomultiplier tube was placed at the bottom of the tube, and an LED with a mean wavelength of 430 nm placed at the top of the tube to act as the light source. This is similar to the experiments performed in Refs. [8, 10, 11].

Using a novel DAQ system with reference to [12], as shown schematically in Fig. 1, two signals with the same frequency are generated by the signal generator. One of the signals is used to trigger the LED to flash. The LED light pulse then travels down the tube containing LAB to the PMT at the bottom of the tube. The generated electronic signal from the PMT is then transmitted to V965, a Dual Range Charge to Amplitude Converter, to convert the PMT signal based on the strength of the attenuated light to an ADC channel value. The other signal from the signal generator is transmitted to V965 via a passive differential circuit, N840 and V993 to form a gate signal. The oscilloscope is used for synchronization regulation between the PMT signal and the gate signal. Using the ADC channel values acquired from the PMT signal, Eq. (1) can be modified to

$$\mathrm{ADC}_x=\alpha \mathrm{ADC}_0 e^{-\frac{x}{L_\lambda}}, \tag{2}$$

where ADC_x is the mean ADC channel value when the liquid height is x, ADC_0 is the ADC channel value when the liquid height is 0.1 m, and α is simply a multiplicative factor due to the fact that we have substituted the initial light intensity-related ADC with an x=0.1 m light intensity-related ADC. In performing the experiment, we measured the mean ADC channel value at 0.1 m intervals beginning from about 1 m in a decreasing manner, i.e. $|\Delta x|$=0.1 m.

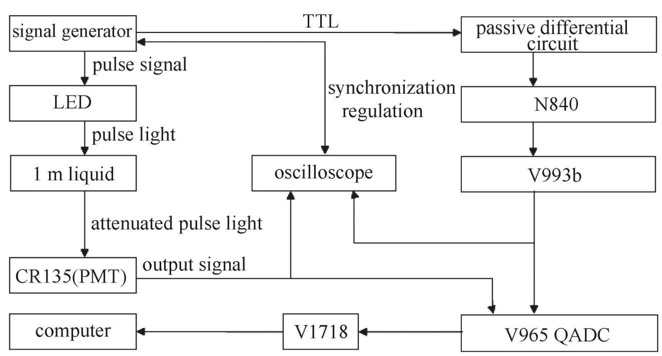

Fig. 1. Schematic diagram of the DAQ system.

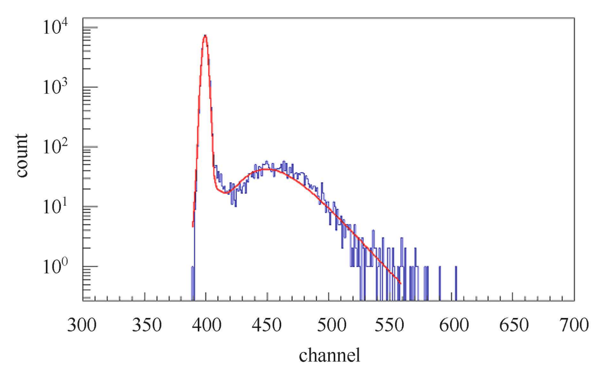

Fig. 2. (color online) Signal from a single photon. The x-axis corresponds to the ADC channel values. Each channel corresponds to 200 fC.

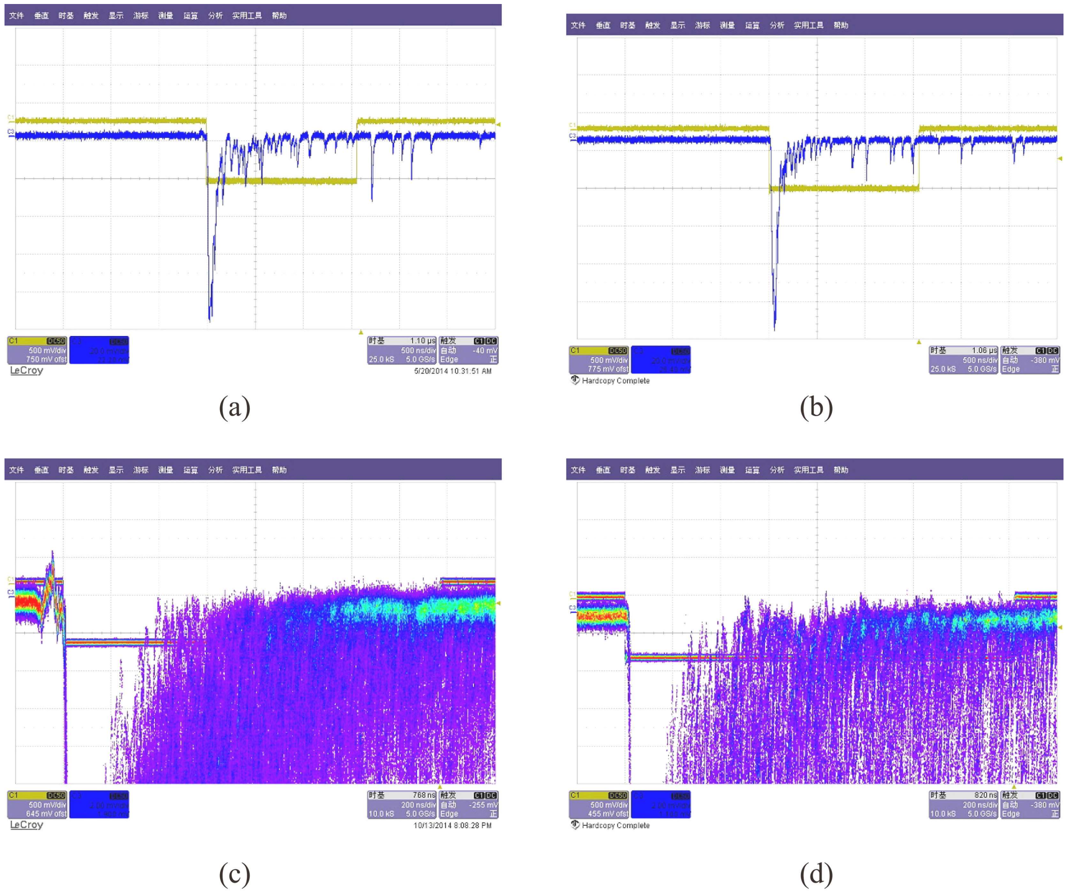

(a) (b) (c) (d)

Fig. 3. (color online) (a) and (c): A scope view of the PMT signal before placing the experimental setup in the clean dark room. (b) and (d): A scope view of the PMT signal after placing the experimental setup in the clean dark room.

For the purpose of finding the optimal PMT applied high voltage, we performed a single photon experiment using the same setup and DAQ system as shown above. The corresponding signal from a single photon is shown in Fig. 2. We found that performing the experiment under a PMT high voltage of 1100 V led to the clearest single photon peak. Such attainability shows that our setup and the DAQ system have a high sensitivity. The data acquisition and transmission rates were determined experimentally. We found, after a large number of trials, that setting the frequency of the signal generator at 800 Hz was the most optimal. Therefore, the PMT high voltage was set to 1100 V and the signal generator frequency was set to 800 Hz throughout the entire experiment for the attenuation length measurements.

3.3 Improvement and upgrade

To reduce the effects of stray light, dust and fluctuations in the ambient temperature on the LED, pulse generator, PMT and electronic readout system, a clean dark room was constructed and placed in our lab, with double-glazed windows. The walls of the room formed a Faraday cage with good ground connection to reduce electromagnetic disturbances to the experiment. Likewise, the PMT signal transmission cables are of shielded types to reduce electromagnetic disturbances. Figure 3(a) and Fig. 3(c) show a PMT signal without having the experimental setup in the clean dark room, in comparison with a signal with the clean dark room as shown in Fig. 3(b) and Fig. 3(d). The usage of our improved setup in the clean dark room has successfully reduced the number and magnitude of after-pulses, as shown in Fig. 3(b) compared to Fig. 3(a). In addition, all pre-pulses have disappeared, as can clearly be seen from Fig. 3(d) compared to Fig. 3(c).

As the PMT signal output has a negative correlation with the ambient temperature, fluctuations in the latter can lead to a large uncertainty in the readout and the measurement of the attenuation length. The relation between the ambient temperature and the ADC value of the PMT signal is shown in Figs. 4 and 5. The results in Fig. 4, taken over a period of four days, were obtained when the experimental setup was not in the dark room. The results in Fig. 5, taken over more than a 10-hour period, were obtained when the experimental setup was placed in the dark room. Figure 4 shows that the temperature can fluctuate within 5 ℃ leading to a 7.5 % fluctuation in the PMT signal output. Figure 5 shows that the temperature fluctuation can be stabilized to below 0.5 ℃ leading to a mere 0.2 % fluctuation in the PMT signal output. This can be observed from the 400 min mark to the 680 min mark in Fig. 5. This stable period was more than sufficient for us to perform the necessary measurements on a LAB sample. Using $\Delta\mathrm{ADC}/\mathrm{ADC}=|\Delta x|/L_{\lambda}$, and that $|\Delta x|=0.1$ m and $\Delta\mathrm{ADC}/\mathrm{ADC}=0.2\%$, an attenuation length L_{λ} of larger than 30 m can be measured in principle.

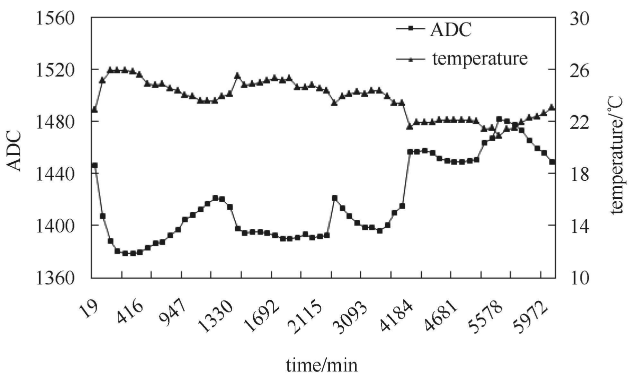

Fig. 4. Change in the ADC value and the ambient temperature when the setup is not placed in a dark room.

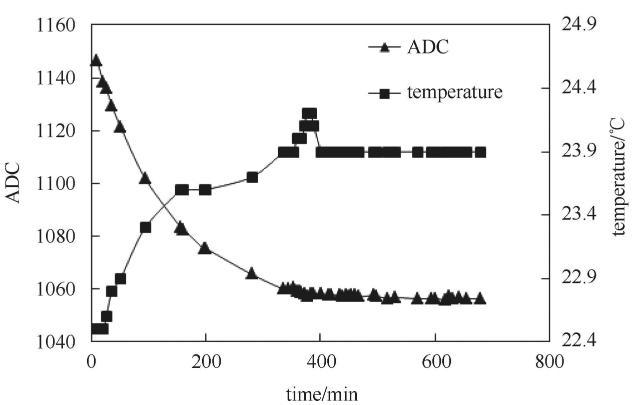

Fig. 5. Change in the ADC value and the ambient temperature when the setup is in a dark room.

4 Results

4.1 Attenuation length measurements of LAB

Figure 6 shows the measurement results of NJ33# based on the usage of different light intensities. The first and second trial were performed with the same light intensity, obtaining similar attenuation lengths within the uncertainty, showing the stability of the experimental setup.

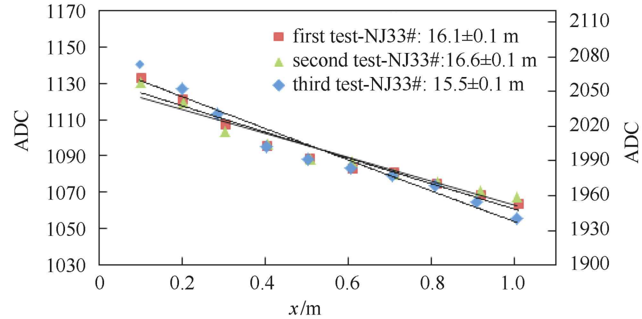

Fig. 6. (color online) Three trials of attenuation length measurements performed with NJ33#. The first and second trial were performed with the same light intensity, while the third trial was performed with a 50% larger light intensity compared to the first and second trial. Included is the attenuation length obtained for each trial from an exponential fit to the data.

Figure 7 shows the measurement results of five LAB samples. Their corresponding attenuation lengths as obtained from the fits to the data are shown in Table 1. An investigation has been made as to whether the method of reducing the liquid height of LAB has any impact on the measurements of the attenuated light intensity. Figure 8 shows the results for NJ32# when the liquid height is reduced in steps of 0.02 m in between the measurement points for attenuated light intensity.

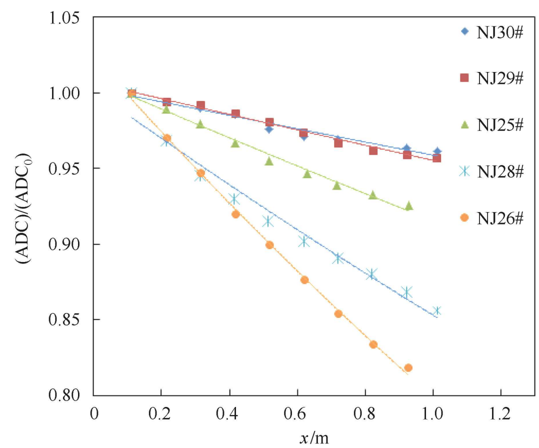

Fig. 7. (color online) ADC/ADC$_0$ of NJ25#, NJ26#, NJ28#, NJ29# and NJ30# for various LAB liquid height x as measured with a low light intensity.

Table 1. Attenuation length of LAB samples.

LAB samples	attenuation length/m
NJ22#	11.2 ± 0.5
NJ25#	10.2 ± 0.1
NJ26#	4.02 ± 0.01
NJ28#	6.19 ± 0.02
NJ29#	19.2 ± 0.2
NJ30#	22.1 ± 0.3

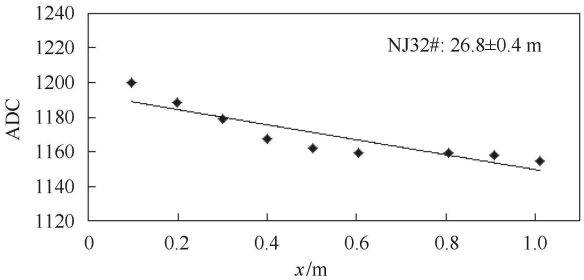

Fig. 8. ADC for NJ32# for various LAB liquid height x, where the reduction in x is done in steps of 0.02 m in between measurement points for attenuated light intensity. The attenuation length obtained from the exponential fit is 26.8 m.

4.2 Inorganic impurities in LAB

Coordination compounds might form due to the existence of inorganic impurities in the LAB samples, which can produce ligand centered (LC) $\pi\rightarrow\pi^*$, metal-to-ligand charge-transfer (MLCT) and metal-to-metal charge-transfer (MMCT) excitations. If the concentration of the inorganic impurities is large, these excitations, which are in the light-absorption range with wavelengths from 350 nm to 550 nm [13, 14], might possibly reduce the attenuation length of the LAB samples in our wavelength of interest. Using the ICP-MS (Thermo X series II) technique, we have made a full spectrum scan of the inorganic impurity content in the LAB samples. The results are shown in Table 2. Elements studied using the ICP-MS technique but not listed in Table 2 were found to have concentrations below the baseline of the technique.

Table 2. Concentration of inorganic impurities in the LAB samples.

	NJ29#	NJ28#	NJ26#
Na/ppb	<0.1	406.1	<0.1
Fe/ppb	<0.1	<0.1	<0.1
Cu/ppb	<0.01	<0.01	<0.01
Zn/ppb	<0.01	<0.11	<0.01
Ru/ppb	<0.01	<0.01	<0.01
Ag/ppb	<0.01	0.02	<0.01
Os/ppb	<0.01	0.23	<0.01
Au/ppb	<0.01	0.04	<0.01

Based on these results, we find that the concentration of inorganic impurities in our LAB samples is so low that any possibility of coordination compounds reducing the attenuation length of LAB is deemed provisionally negligible.

4.3 C/H ratio of LAB

Gd has been used in past detectors, including Daya Bay, for enhancement of neutron capture [15]. In view of a tentative plan by JUNO to use an LS liquid without the addition of Gd, based on a new analysis by the Daya Bay collaboration on the possibility of neutron capture with hydrogen [16], we have also done a study on the C/H ratio of our LAB samples. The hope is to find a suitable low C/H ratio liquid scintillator with excellent light transparent properties, including large attenuation length, for use in the JUNO experiment.

Table 3 shows the C/H ratio as obtained through an Element Analysis technique (CHN-O-Rapid type) and the attenuation length for the LAB samples produced by Jinling. Among the LAB samples that have been studied, the attenuation length of NJ30# is the largest, and at the same time, the said sample also has the lowest C/H ratio compared to the other LAB samples.

Table 3. C/H ratio and attenuation length of the LAB samples.

	attenuation length/m	C/H ratio
NJ30#	22.1 ± 0.3	7.109
NJ28#	6.19 ± 0.02	7.171
NJ26#	4.02 ± 0.01	7.113
NJ25#	10.2 ± 0.1	7.129
NJ22#	11.2 ± 0.5	7.414

5 Discussion

In the attenuation length measurement experiment, it can be observed from Fig. 6 that a high light intensity can lead to deviations from Eq. (1). This suggests that the PMT might have effectively lost its linearity property at this intensity magnitude.

In Fig. 8, where the liquid height was reduced in small steps (in this case, 0.02 m) until the next desired height to be measured for its corresponding attenuated light intensity, the data for NJ32# is not well-fitted with an exponential curve that is consistent with Eq. (2), but nonetheless, shows the largest attenuation length that has been measured from our samples yet. In comparison, we observe a better agreement between the data and Eq. (2) in Figs. 6 and 7, where the liquid height was reduced in one full step. Investigation into the cause of this is still in progress.

Overall, the concentration of the impurities in the LAB samples was sufficiently low. Even if the influence on the attenuation length of LAB by inorganic impurities is currently negligible, the case for organic impurities playing an important role in reducing the attenuation length of LAB samples still has to be investigated deeply. In particular, we will be interested in identifying the functional groups among the organic impurities with the largest impact on the attenuation length.

6 Summary

In this work, the light absorption properties of different LAB samples have been studied. The attenuation lengths of the samples have been quantified with measurements performed in a clean dark room under a less than 0.5 °C ambient temperature fluctuation with an acquired PMT signal stable to within 0.2 %. Furthermore, the inorganic impurity content of the samples has been found to be negligible, and thus, we find no evidence that inorganic impurities have any significant impact on the attenuation length of the samples. The C/H ratio has been obtained for different LAB samples. We find that it is possible to prepare a LAB sample with large attenuation length while having a low C/H ratio. In addition, further study on the light absorption properties of LAB and improvement of the measurement techniques thereof is in progress.

We are grateful for many helpful discussions and suggestions, including from Chen Shen-Jian, Wang Yi-Fang, Cao Jun, Heng Yue-Kun, Qian Sen, Zhou Li, Ding Ya-Yun, Yu Bo-Xiang, Ning Zhe and Xia Jing-Kai.

References

1 JUNO Collaboration, JUNO CDR, edited by JUNO Collaboration (2014), p.6
2 L. Zhan, Y. F. Wang, J. Cao et al, Physical Review D, **78**: 111103(R) (2008)
3 L. Zhan, Y. F. Wang, J. Cao et al, Physical Review D, **79**: 073007 (2009)
4 Y. F. Li, J. Cao, Y. F. Wang et al, Physical Review D, **88**: 013008 (2013)
5 F. P. An et al (Daya Bay Collaboration), Phys. Rev. Lett., **108**: 171803 (2012)
6 G. Johnny, N. James, M. F. Yeh et al, Nuclear Instruments and Methods in Physics Research A, **637**: 47–52 (2011)
7 Y. Y. Ding, Z. Y. Zhang, J. C. Liu et al, Nuclear Instruments and Methods in Physics Research A, **584**: 238–243 (2008)
8 P. Huang, P. Li, Z. Fu et al, JINST, **5**: P08007 (2010)
9 P. W. Huang, H. Y. Cao, M. Qi et al, Theor. Chem. Acc., **129**: 229–234 (2011)
10 P. Y. Li, P. W. Huang, Z. W. Fu et al, Nuclear Techniques, **33**(8): 636–640 (2010) (in Chinese)
11 J. C. Liu, Z. H. Li, C. G. Yang et al, High Energy Physics and Nuclear Physics, **31**(1): 76–79 (2007) (in Chinese)
12 Z. Ning, S. Qian, Z. W. Fu et al, Nuclear Techniques, **33**(10): 740–744 (2010) (in Chinese)
13 D. H. Oh, M. Sano, S. G. Boxer et al, J. Am. Chem. Soc., **113**: 6880–6890 (1991)
14 M. G. Colombo, A. Hauser, and H. U. Gudel, Inorg. Chem., **32**: 3088–3092 (1993)
15 W. Beriguete, J. Cao, Y. Y. Ding et al, Nuclear Instruments and Methods in Physics Research A, **763**: 82–88 (2014)
16 F. P. An et al (Daya Bay Collaboration), Phys. Rev. D, **90**: 071101 (2014)